Richard Bland Faculty Works

Richard Bland College

2-2020

FTY720/fingolimod decreases hepatic steatosis and expression of fatty acid synthase in diet-induced nonalcoholic fatty liver disease in mice

Timothy D. Rohrbach
Richard Bland College of the College of William and Mary, trohrbach@rbc.edu

Amon Asgharpour

Melizza A. Maczis

David Montefusco

Ashley Cowart

See next page for additional authors

Follow this and additional works at: https://scholarworks.wm.edu/rbc_facwork

Part of the Biology Commons

Authors

Timothy D. Rohrbach, Amon Asgharpour, Melizza A. Maczis, David Montefusco, Ashley Cowart, Pierre Bedossa, Arun J. Sanyal, and Sarah Spiegel

FTY720/fingolimod decreases hepatic steatosis and expression of fatty acid synthase in diet-induced nonalcoholic fatty liver disease in mice

Timothy D. Rohrbach,* Amon Asgharpour,[†,§] Melissa A. Maczis,* David Montefusco,*
L. Ashley Cowart,*,** Pierre Bedossa,[††] Arun J. Sanyal,[†] and Sarah Spiegel[1],*

Department of Biochemistry and Molecular Biology* and Division of Gastroenterology, Hepatology, and Nutrition,[†] Department of Internal Medicine, Virginia Commonwealth University School of Medicine, Richmond, VA; Division of Liver Diseases,[§] Icahn School of Medicine at Mount Sinai, New York, NY; Hunter Holmes McGuire Veterans Administration Medical Center,** Richmond, VA; and Liverpat,[††] Paris, France

Abstract Nonalcoholic fatty liver disease (NAFLD), a leading cause of liver dysfunction, is a metabolic disease that begins with steatosis. Sphingolipid metabolites, particularly ceramide and sphingosine-1-phosphate (S1P), have recently received attention for their potential roles in insulin resistance and hepatic steatosis. FTY720/fingolimod, a prodrug for the treatment of multiple sclerosis, is phosphorylated in vivo to its active phosphorylated form by sphingosine kinase 2 and has been shown to interfere with the actions of S1P and to inhibit ceramide biosynthesis. Therefore, in this study we investigated the effects of FTY720 in a diet-induced animal model of NAFLD (DIAMOND) that recapitulates the hallmarks of the human disease. The oral administration of FTY720 to these mice fed a high-fat diet and sugar water improved glucose tolerance and reduced steatosis. In addition to decreasing liver triglycerides, FTY720 also reduced hepatic sphingolipid levels, including ceramides, monohexosylceramides, and sphingomyelins, particularly the C16:0 and C24:1 species, as well as S1P and dihydro-S1P. FTY720 administration decreased diet-induced fatty acid synthase (FASN) expression in DIAMOND mice without affecting other key enzymes in lipogenesis. FTY720 had no effect on the expression of SREBP-1c, which transcriptionally activates FASN. However, in agreement with the notion that the active phosphorylated form of FTY720 is an inhibitor of histone deacetylases, FTY720-P accumulated in the liver, and histone H3K9 acetylation was markedly increased in these mice. Hence, FTY720 might be useful for attenuating FASN expression and triglyceride accumulation associated with steatosis.—Rohrbach, T. D., A. Asgharpour, M. A. Maczis, D. Montefusco, L. A. Cowart, P. Bedossa, A. J. Sanyal, and S. Spiegel. **FTY720/fingolimod decreases hepatic steatosis and expression of fatty acid synthase in diet-induced nonalcoholic fatty liver disease in mice.** *J. Lipid Res.* 2019. **60:** 1311–1322.

Supplementary key words lipogenesis • sphingolipids • sphingosine-1-phosphate

Nonalcoholic fatty liver disease (NAFLD) encompasses a spectrum of disease states defined by hepatic steatosis occurring in the absence of alcohol abuse (1). Steatosis is the initial stage of NAFLD, in which lipid droplets form and accumulate in the liver (2). This stage can be self-limiting; however, steatosis can progress to more aggressive liver injury, inflammation, and fibrosis in the form of nonalcoholic steatohepatitis (NASH) (3). NASH can progress to cirrhosis, end-stage liver disease, or hepatocellular carcinoma (4). Caloric excess, associated with obesity, insulin resistance, and dyslipidemia, has been implicated in the development of NAFLD (5), and it is estimated that about a third of the US population has NAFLD (6). Approximately 30% to 50% of NAFLD patients have NASH at the time of diagnosis (7) and, unfortunately, however, there are currently no approved therapies (8).

The oversupply of nutrients due to obesogenic diet consumption alters many aspects of cellular metabolism, including the biosynthesis of lipids (9). Several lipid mediators typically associated with lipotoxicity, such as diacylglycerols, free fatty acids, oxysterols, and more recently, sphingolipids, have been linked to the progression of steatosis to NASH (9–11). It has been suggested that the bioactive sphingolipid ceramide contributes to insulin

Abbreviations: CD, chow diet; CerS, ceramide synthase; FASN, fatty acid synthase; HDAC, histone deacetylase; HFD, high-fat diet; NAFLD, nonalcoholic fatty liver disease; NASH, nonalcoholic steatohepatitis; S1P, sphingosine-1-phosphate; SW, sugar water; WD, Western diet.
[1] To whom correspondence should be addressed.
 e-mail: sarah.spiegel@vcuhealth.org

resistance, enhanced hepatic inflammation, and fibrosis and is involved in the development of NASH (12–15). The genetic or pharmacological inhibition of ceramide biosynthesis in mouse models of obesity decreased insulin resistance and hepatic steatosis (16–20). The manipulation of the ceramide synthase (CerS) isoforms 2, 5, and 6 suggests that ceramides composed of long side chains, particularly C16:0, play an important role in obesity-induced insulin resistance, glucose intolerance, steatohepatitis, and adipose tissue inflammation (18–20). Furthermore, a positive association between ceramides containing saturated side chains and insulin resistance that is independent of triglycerides has been reported in humans (11, 21).

Levels of the ceramide metabolite sphingosine-1-phosphate (S1P) produced by two sphingosine kinase isoenzymes, SphK1 and SphK2, were also elevated in the livers of mice fed a high-fat diet (HFD) (22). Moreover, the SphK1/S1P axis was shown to mediate hepatic inflammation in a mouse model of NASH induced by high-saturated-fat feeding (23), suggesting that enhanced S1P levels in the circulation may mediate some of the systemic effects associated with HFD and obesity (15). Furthermore, increases in plasma S1P in obese humans correlated with fasting plasma insulin level, body fat percentage, and body mass index (24).

To improve understanding of the development of NAFLD and provide insights into future therapeutic avenues, many animal models have been studied (25). However, most do not exhibit the full spectrum of features associated with human NASH (25). A diet-induced animal model of NAFLD (DIAMOND) that recapitulates the key physiological, metabolic, histologic, transcriptomic, and cell-signaling changes seen in humans with progressive NASH has recently been developed (26). DIAMOND is a useful preclinical approach for developing better diagnostic and therapeutic strategies for patients with NASH, targeting those with early-stage disease as well as those with advanced liver fibrosis (27). To better understand the involvement of ceramide and its metabolites in the development of the disease, we used FTY720/fingolimod, an orally available immunosuppressive drug used for treating multiple sclerosis (28) that has been shown to inhibit CerS in vitro (29, 30). FTY720 also inhibits de novo ceramide biosynthesis in cultured cells (30, 31) and mice (32, 33). In addition, FTY720 inhibits and reduces levels of SphK1 and S1P (34, 35). Our results suggest that FTY720 could have beneficial effects on the early stage of disease development.

MATERIALS AND METHODS

Animals

Isogenic mice derived from C57BL/6J and 129S1/SvImJ backgrounds (B6/129) were kindly provided by Dr. Sandra Erickson (UCSF) and maintained by inbreeding as previously described (26). The mice were housed under a 12-h light/12-h dark cycle in a 21–23°C facility. All procedures were approved by the Animal Care and Use Committee of Virginia Commonwealth University.

Diet and treatments

Genome-wide association mapping of hepatic triglycerides revealed striking differences in the genetic control of hepatic steatosis between female and male mice (36). Female mice were used for this study because the reduced severity of HFD-induced NAFLD in female mice precludes the interrogation of disease pathogenesis in a sex-independent manner. Female mice were fed a standard chow diet (CD; Harlan TD.7012) until reaching 12 weeks of age unless indicated otherwise. Mice were then fed a high-fat, high-carbohydrate diet (Harlan TD.88137) containing 42% kcal from milk fat and 0.1% cholesterol (Western diet; WD) for 16 weeks. Drinking water contained a high amount of fructose (23.1 g/l) and glucose (18.9 g/l) (sugar water; SW) (26). Both food and water were provided ad libitum. FTY720/fingolimod (0.3 mg/kg; Cayman Chemical #10006292) or vehicle (saline) was administered via oral gavage three times a week throughout the 16-week HFD. Where indicated, control mice were fed a standard CD (Harlan TD.7012) with normal drinking water.

Pathology

Mice were weighed and euthanized with inhaled isoflurane and cervical dislocation. Livers were removed, and a portion was sectioned for formalin fixation and histological processing. The remaining liver was placed in cryotubes and snap-frozen in liquid nitrogen. Formalin-fixed and paraffin-embedded liver slices were stained with H&E. Liver fibrosis was examined by staining with Masson's trichrome and Sirus Red (37). An expert liver pathologist evaluated the liver histology in a treatment-blinded manner. The NASH-Clinical Research Network scoring system was used to score steatosis, lobular inflammation, and hepatocellular ballooning as previously described (26, 38). Steatosis (percentage hepatocytes with fat droplets) was scored as 0 (<0.5%), 1 (5–33%), 2 (>33–66%) or 3 (>66%). Hepatocyte ballooning was scored as 0 (none), 1 (few cells), or 2 (many cells). Lobular inflammation was scored as 0 (no foci), 1 (<2 foci per field), 2 (2–4 foci), or 3 (>4 foci). Steatosis, inflammation, and ballooning scores were combined for the NAFLD activity score. Fibrosis was also evaluated as stage F0 (none), F1 (mild), F2 (perisinusoidal and portal/periportal fibrosis), F3 (bridging fibrosis), or F4 (obvious cirrhosis).

Glucose tolerance and insulin tolerance tests

Mice were fasted overnight, and baseline blood glucose levels were measured in tail-vein blood. Glucose (1 mg dextrose/kg body weight) dissolved in sterile PBS was injected intraperitoneally. Blood glucose levels were then determined at 15, 30, 60, 90, and 120 min postglucose injection. All glucose measurements were determined with an Accu-Chek Compact plus glucometer (Roche Diagnostics), and areas under the curve were determined (39). Repeat glucose tolerance tests were performed after several days. For the insulin tolerance test, mice were injected intraperitoneally with insulin (0.75 U/kg body weight), and blood glucose levels were measured prior to and 30 and 60 min after insulin injection.

Immunoblotting

Liver tissues were pulverized in liquid nitrogen and then lysed in buffer containing 50 mM HEPES, pH 7.4, 150 mM NaCl, 100 mM NaF, 10% glycerol, 10 mM sodium pyrophosphate, 200 μM sodium vanadate, 10 mM EDTA, and 1% Triton X-100 supplemented with Halt Protease and Phosphatase Inhibitor Cocktail (#78446, Thermo Fisher Scientific). Proteins were separated on 10% SDS-PAGE and transferred to nitrocellulose membranes (Immun-Blot, #1620115; Bio-Rad). Membranes were blocked with 5% BSA-TBST and incubated overnight with fatty acid synthase (#3189); (FASN) and β-actin (Cell Signaling) (#4967).
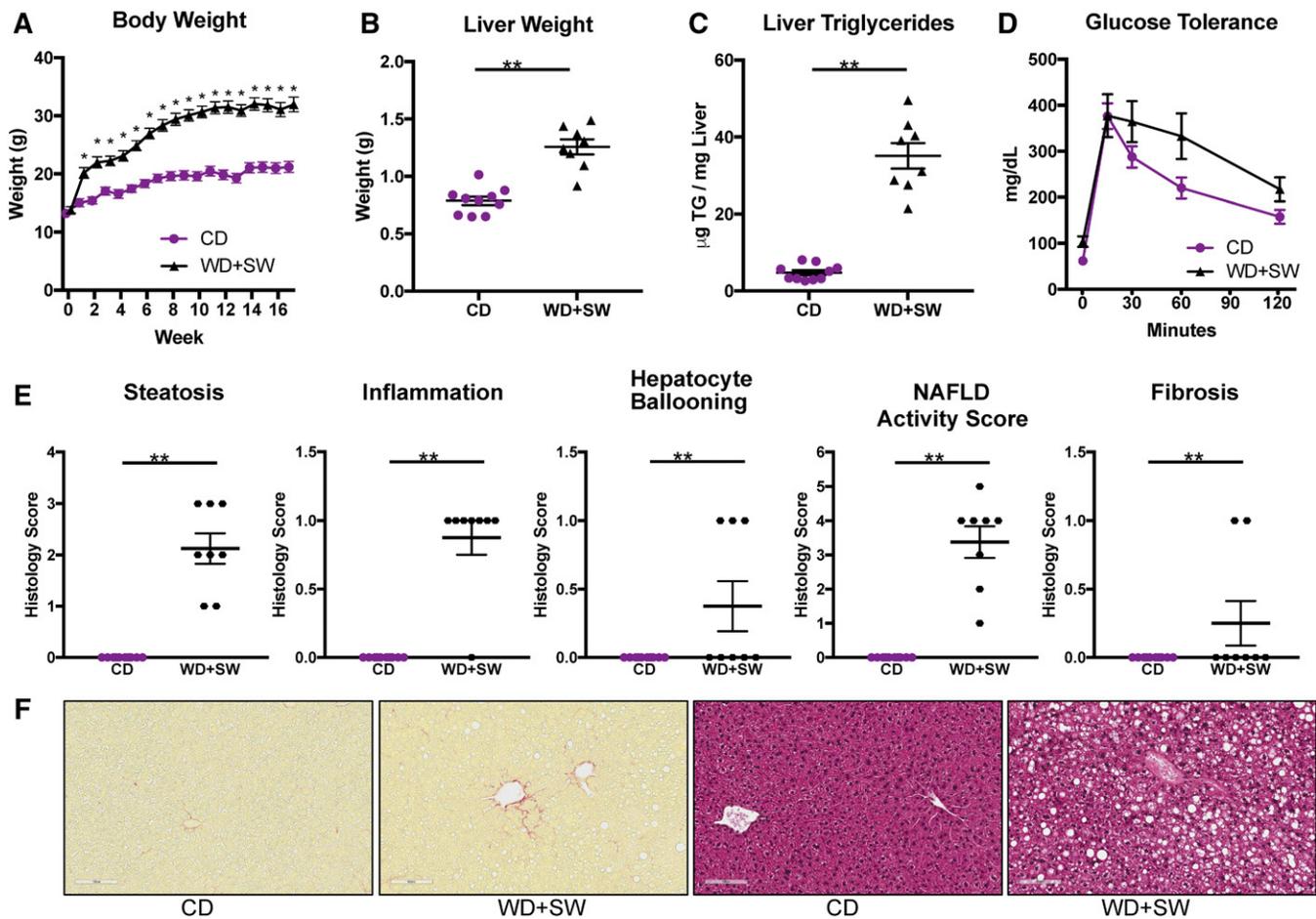
Fig. 1. Mice on a WD supplemented with SW develop obesity, fatty livers, inflammation, liver fibrosis, and steatosis. B6/129 female mice were fed a CD or WD with SW for 16 weeks. Mice were 12 weeks old at the beginning of feeding the WD + SW ($n = 10$), whereas the control mice group fed the CD consisted of 4 mice that were 10 weeks old and 6 that were 12 weeks old. A: Body weight. B: Liver weight. C: Hepatic triglycerides levels. D: Glucose tolerance tests. E: Histology scores for liver steatosis, inflammation, hepatocyte ballooning, NAFLD activity score, and fibrosis. F: Representative images of liver sections stained with H&E or Picrosirius red. Size bars: 10 μm. Data are expressed as means ± SEMs, $n = 8$–10 mice per group. *$P < 0.01$ and **$P < 0.001$.

Immunopositive bands were visualized by incubation with HRP-conjugated secondary antibodies (1:5000 dilution; Jackson ImmunoResearch) for 1 h at room temperature before adding SuperSignal West Pico chemiluminescence substrate (#34080, Thermo Fisher Scientific). Blots were quantified with ImageJ and normalized to their corresponding loading controls.

Nuclear extracts

Livers were homogenized in buffer containing 10 mM HEPES, pH 7.8, 10 mM KCl, 0.1 mM EDTA, 1 mM Na_3VO_4, 1 mM DTT, and phosphatase and protease inhibitor cocktail (Thermo Fisher Scientific) and incubated on ice for 15 min. NP-40 was added to a final concentration of 0.75% (v/v), and the tissue suspension was vortexed for 10 s and then incubated on ice for 4 min. Nuclear and cytoplasmic fractions were separated by centrifugation at 3,000 *g* for 4 min at 4°C. Nuclei were resuspended in high-salt buffer containing 20 mM HEPES, pH 7.8, 0.4 M NaCl, 1 mM EDTA, 1 mM Na_3VO_4, 1 mM DTT, and 1:500 phosphatase and protease inhibitors, sonicated on ice, and incubated on ice for 5 min. Nuclear extracts were cleared by centrifugation at 3,000 *g* for 5 min at 4°C. Proteins were separated by SDS-PAGE, transblotted to nitrocellulose, and incubated with primary antibodies as indicated in the figure legends, including rabbit polyclonal antibodies to histone H3-K9ac (1:1000; AbCam) and histone H3 (1:1000; Cell Signaling).

RNA analysis

RNA was extracted from liver tissues with TRIzol Reagent (15596-018, Ambion, Thermo Fisher Scientific). RNA (2 μg) was treated with RQ1 DNase (M6101, Promega) and converted by the High-Capacity cDNA Reverse Transcription Kit (4368814, Thermo Fisher Scientific) to cDNA. SYBR Green PCR Master Mix (Thermo Fisher Scientific) was mixed with the Bio-Rad mouse primers gapdh (CED0027497) and fasn (CID0015083). Reactions were analyzed with the use of the CFX Connect Real-Time PCR Detection System (Bio-Rad) (40). Gene expression levels were calculated by the $\Delta\Delta C_t$ method and normalized to GAPDH expression.

Blood collection and analysis

Blood was collected from hepatic veins, and serum was obtained by centrifugation for 15 min at 1,500 *g* at 4°C. Serum alanine aminotransferase, aspartate aminotransferase, cholesterol, HDL, LDL, and triglycerides were measured by the Virginia Commonwealth University Hospital Department of Pathology.

Sphingolipid measurements

Lipids were extracted from liver tissue and whole blood, and sphingolipids were quantified by LC/ESI/MS/MS (AB Sciex 5500) as previously described (41).
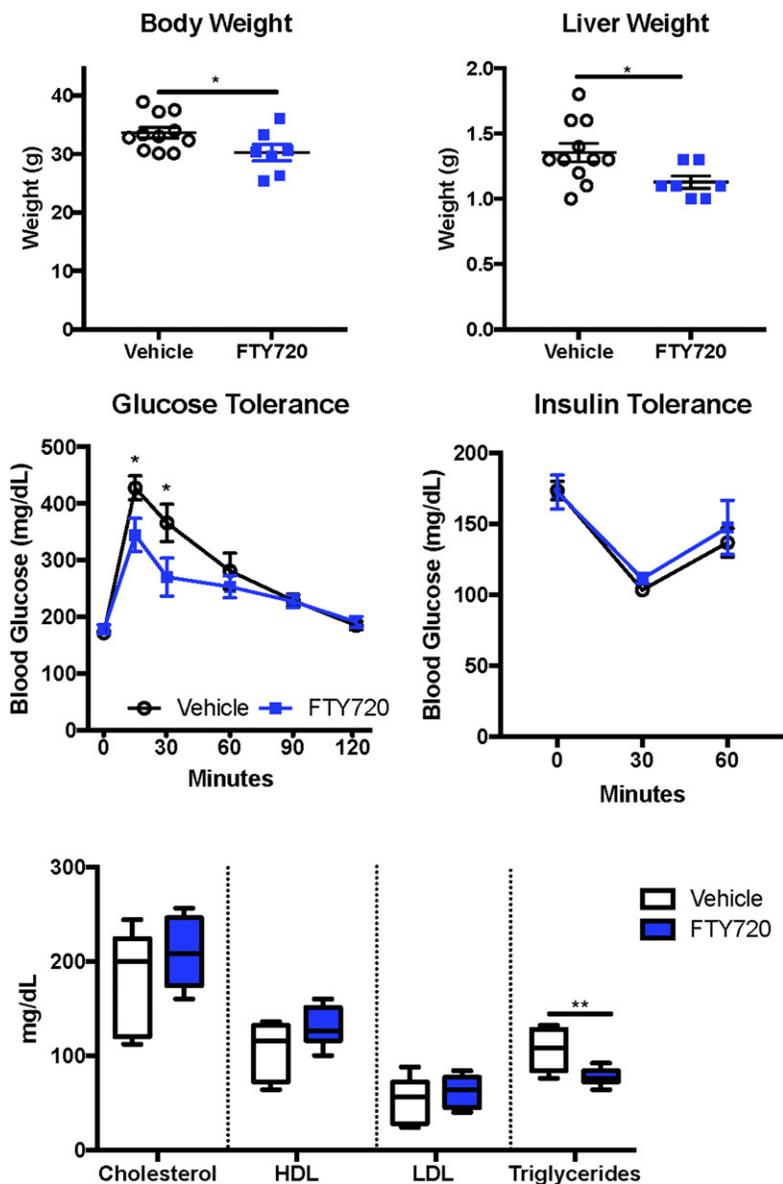
Fig. 2. FTY720 administration reduced liver weight and improved glucose tolerance and triglycerides in mice fed a WD supplemented with SW. B6/129 female mice fed a WD with SW for 16 weeks were treated 3 times per week with vehicle or 0.3 mg/kg FTY720 by oral gavage. A: Body weight. B: Liver weight. C: Glucose tolerance test. D: Insulin tolerance test. E: Serum cholesterol, HDL, LDL, and triglycerides levels. Data are expressed as means ± SEMs, n = 7–10 mice per group. *$P < 0.05$ and **$P < 0.005$.

Statistics

Statistical significance was determined with unpaired two-tailed Student's t-tests for comparisons of two groups or by ANOVA followed by post hoc tests for multiple comparisons (GraphPad Prism). $P < 0.05$ was used to indicate statistical significance.

RESULTS

DIAMOND mice develop obesity, fatty liver, dyslipidemia, and steatohepatitis

Previous studies demonstrated that feeding B6/129 mice an HFD supplemented with SW mimics a typical WD (42) and triggers NASH development (26). In agreement, we observed that when female B6/129 mice were fed a WD with 42% calories from fat together with drinking water containing fructose and glucose (SW) for 16 weeks they rapidly gained weight (**Fig. 1A**), leading to increased liver weight (Fig. 1B) and accumulation of hepatic triglycerides (Fig. 1C)

compared with mice fed a CD. Similar to previous studies (26), glucose tolerance tests showed that glucose levels were higher following intraperitoneal glucose administration in mice fed a WD with SW, although it was not statistically significant (Fig. 1D). As expected, liver histology indicated that these mice also developed fatty livers, with extensive macrovesicles and small droplets (Fig. 1F), indicative of steatosis (Fig. 1E) and consistent with the increased levels of hepatic triglycerides (Fig. 1C). Extensive steatohepatitis was also characterized by increased lobular inflammation and hepatocellular ballooning, all leading to an increased NAFLD activity score (Fig. 1E). Staining with PicoSirius Red to visualize collagen fibers (fibrosis) in liver sections revealed only a small pericellular sinusoidal fibrosis (Fig. 1E, F), suggesting that fibrosis had not yet developed significantly.

FTY720 improved glucose tolerance and reduced steatosis in DIAMOND mice

Previous studies have shown that FTY720 reduced muscle lipid accumulation and improved glucose tolerance in
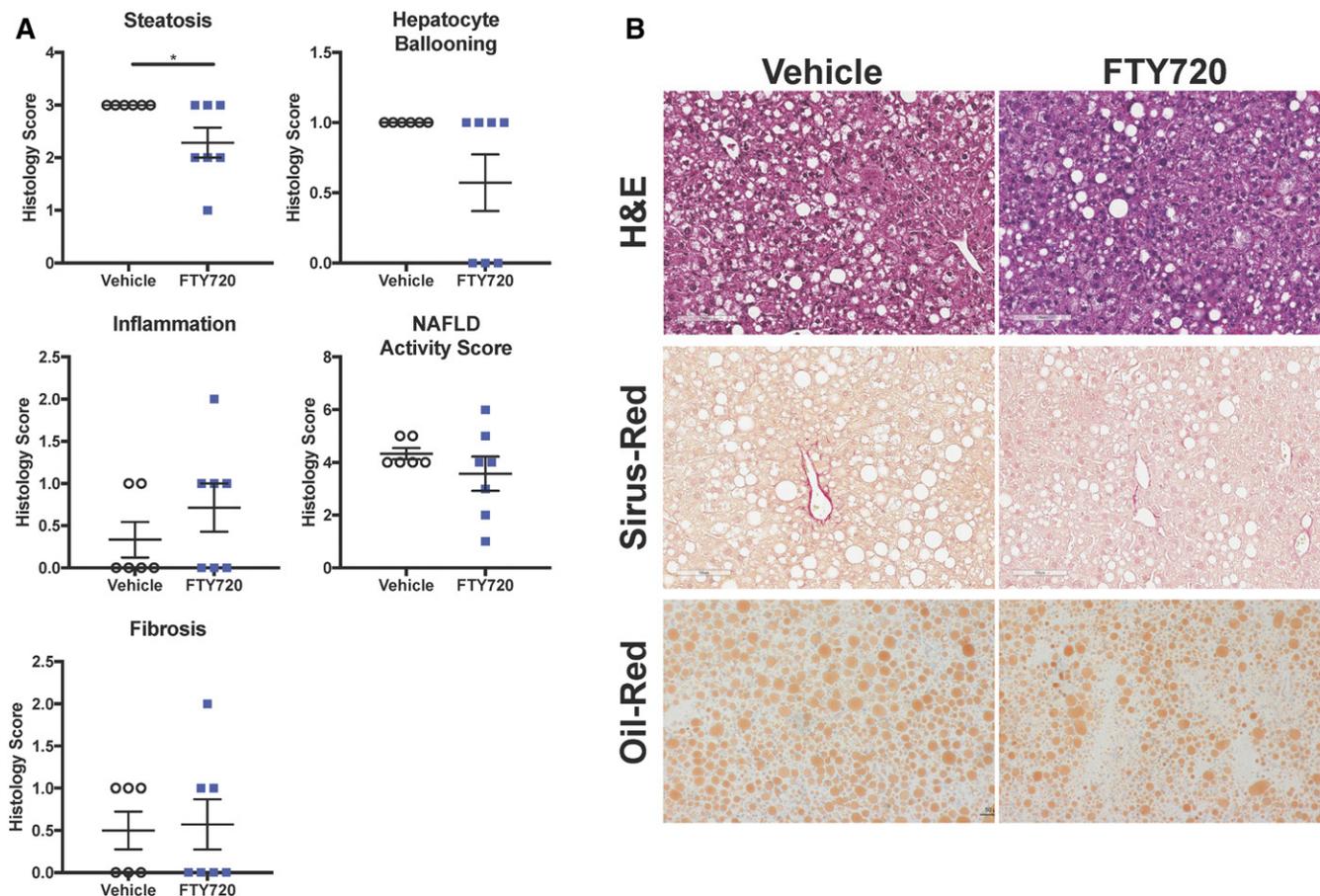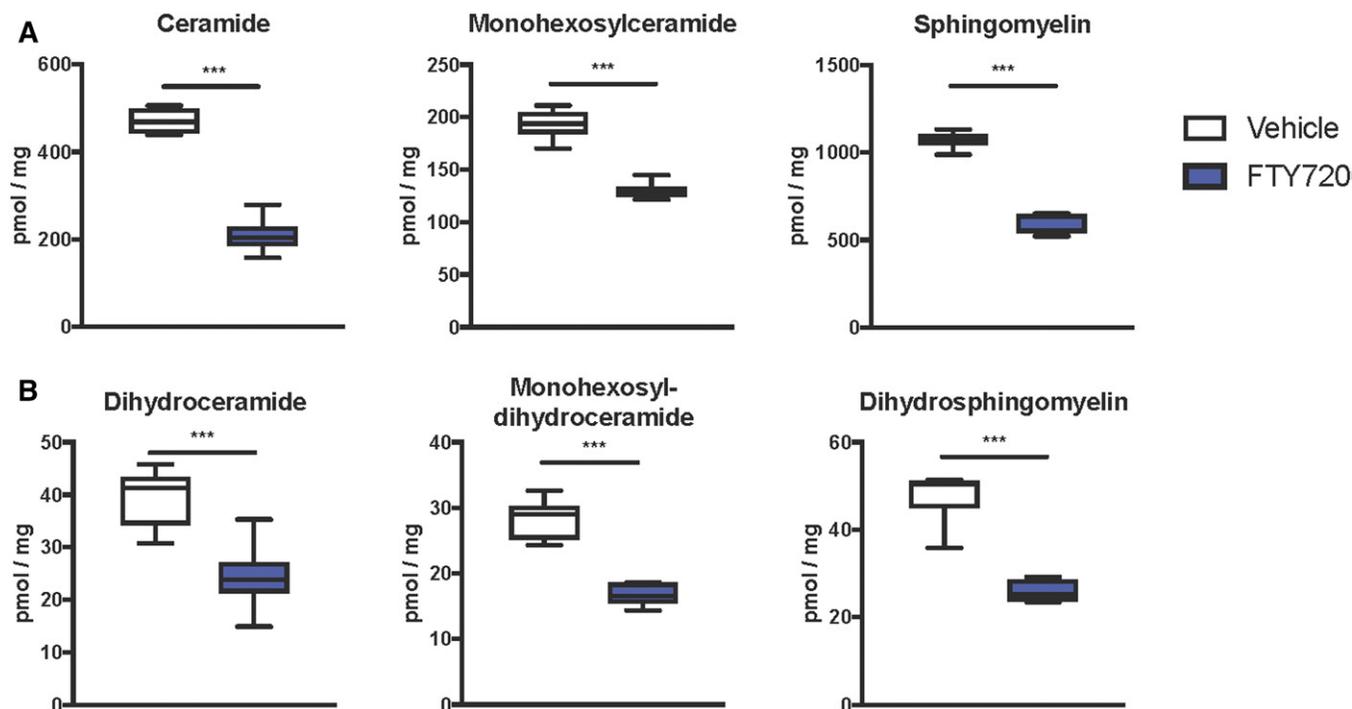
Fig. 3. FTY720 administration reduced steatosis in DIAMOND mice. Mice were fed and treated as described in Fig. 2. A: Histology scores for liver steatosis, inflammation, hepatocyte ballooning, NAFLD activity score, and fibrosis. B: Representative images of liver sections stained with H&E, Picrosirius red, and oil red. Size bars: 100 μm. Data are expressed as means ± SEMs, $n = 8$ mice per group. *$P < 0.05$.

mice fed an HFD (43). However, the dose of FTY720 used in this study was too high to be clinically relevant in humans. Because our results support the notion that B6/129 mice fed a WD with SW for 16 weeks is indeed an excellent model for studying the early development of steatohepatitis (26), it was of interest to examine the effects of a lower, clinically relevant dose of FTY720 in DIAMOND mice. Orally administered 0.3 mg/kg FTY720 three times per week slightly reduced body weight (**Fig. 2A**) and significantly reduced liver weight (Fig. 2B) without affecting spleen weight (data not shown) in mice fed an HFD with SW for 16 weeks. FTY720 improved glucose tolerance and decreased the area under the curve by 13.7% (Fig. 2C). However, DIAMOND mice remained insulin-sensitive at 16 weeks, as assessed with an insulin tolerance test, and FTY720 administration had no significant effects (Fig. 2C). Although there were no major changes in circulating levels of cholesterol or in HDL or LDL, there was a small but significant reduction in circulating triglyceride levels (Fig. 2D). The assessment of NAFLD severity in a blinded manner in these mice revealed that treatment with FTY720 also significantly reduced steatosis compared with mice treated with saline (vehicle) (**Fig. 3A**). However, there were no significant changes in hepatic inflammation, hepatocyte ballooning, NAFLD activity score, or fibrosis scoring after

FTY720 treatment (Fig. 3A, B). Consistent with a 27% reduction in circulating triglycerides (Fig. 2D), FTY720 also reduced the size and number of lipid droplets in liver sections (Fig. 3B), and there was a small reduction in oil red staining used to visualize neutral triglycerides.

FTY720 treatment decreased hepatic sphingolipids

Because it has been suggested that ceramides and S1P may contribute to the development of NAFLD (13–15, 44) and FTY720 can reduce sphingolipid biosynthesis in vivo (32, 33, 43), we next examined the effects of FTY720 administration on hepatic sphingolipids. MS analyses showed that FTY720 significantly decreased levels of all classes of liver sphingolipids examined, including ceramides, monohexosylceramides, and sphingomyelins (**Fig. 4A**). Moreover, dihydroceramides, monohexosyldihydroceramides, and dihydrosphingomyelins, which mainly come from de novo sphingolipid synthesis, were also lower in mice treated with FTY720 compared with mice treated with vehicle (Fig. 4B). These decreases were especially robust in C16:0 and C24:1 species, although almost all chain lengths were significantly reduced (**Fig. 5**). Interestingly, although levels of S1P as well as dihydro-S1P were also significantly decreased in livers from mice that received FTY720, no concomitant increases were noted in levels of their precursors sphingosine

Fig. 4. FTY720 administration reduces hepatic sphingolipid levels. Mice were fed and treated as described in Fig. 2. Lipids were extracted from livers and ceramides, monohexosylceramides, and sphingomyelins (A), as well as their dihydro counterparts (B) measured by LC/ESI/MS/MS. Data are total sphingolipid levels and are shown as box and whisker plots, n = 6–11 mice per group. ***P < 0.005.

or dihydrosphingosine (**Fig. 6**), probably due to the much lower relative levels of the phosphorylated bases.

Because previous studies have suggested that CerS5 (20) and/or CerS6 (18) are important in maintaining C16:0-ceramide pools that contribute to the development of diet-induced obesity and glucose intolerance, we next examined the effect of FTY720 on hepatic CerS expression. However, despite significant decreases in liver sphingolipids and ceramides, hepatic mRNA expression of the six CerS isozymes involved in the biosynthesis of ceramides was not significantly altered by FTY720 administration (**Fig. 7A**).

In addition to inhibiting ceramide synthesis, it is well established that FTY720 is a prodrug that is phosphorylated in vivo by SphK2 to the active FTY720-P that binds to all of the S1PRs except S1PR2 and modulates their actions (28). Therefore, we examined the expression of these receptors in livers isolated from DIAMOND mice fed a WD + SW treated without or with FTY720. In agreement with a previous study (45), S1pr1-3 were predominantly expressed, while S1pr4 and S1pr5 levels were below detection limits (Fig. 7B). However, FTY720 administration did not significantly affect the expression of either the S1P receptors (*S1pr1-3*), nor did it affect the expression of *Sphk1* or *Sphk2* (Fig. 7B). As previous studies suggest that FTY720 reduces macrophage-associated liver inflammation (46), we also examined the effect of FTY720 on proinflammatory cytokine and chemokine expression. However, 16 weeks after feeding a WD + SW, metabolic perturbation predominated and lobular inflammation was just beginning (Fig. 1). FTY720 treatment decreased, albeit not statistically significantly, the proinflammatory cytokine TNF-α, which has been shown

to increase in the progression of NAFLD to inflammatory NASH and cirrhosis (47) (Fig. 7C). Yet there were no effects on the expression of another proinflammatory cytokine, IL-6. Moreover, although the hepatic expression of two key monocyte-attracting chemokines, CCL2, also known as monocyte chemotactic protein 1, and CCL3, macrophage inflammatory protein 1-α, were not significantly altered by FTY720 administration, there were significant reductions in the expression of CXCL10, also known as interferon γ-induced protein 10, a known chemoattractant for monocytes/macrophages, T-cells, and dendritic cells (Fig. 7C). Likewise, the expression of CCL5, also known as RANTES (regulated on activation, normal T-cell expressed and secreted), that plays an active role in the recruitment of leukocytes was also reduced by FTY720 (Fig. 7C).

FTY720 administration decreased HFD-induced FASN expression in DIAMOND mice

To better understand the mechanism by which FTY720 suppresses the development of steatosis, liver levels of mRNA encoding key enzymes involved in lipogenesis and lipid metabolism were determined by quantitative PCR. We particularly focused on genes whose expression levels have been shown to be elevated in the early phase of steatosis induced in DIAMOND mice (48) and are also hallmarks of NAFLD in humans (48). Surprisingly, FTY720 treatment did not significantly affect the expression of many of these genes, including sterol regulatory element binding transcription factor 1 (Srebp-1c), a transcription factor involved in sterol biosynthesis; farnesoid X receptor, an essential regulator of
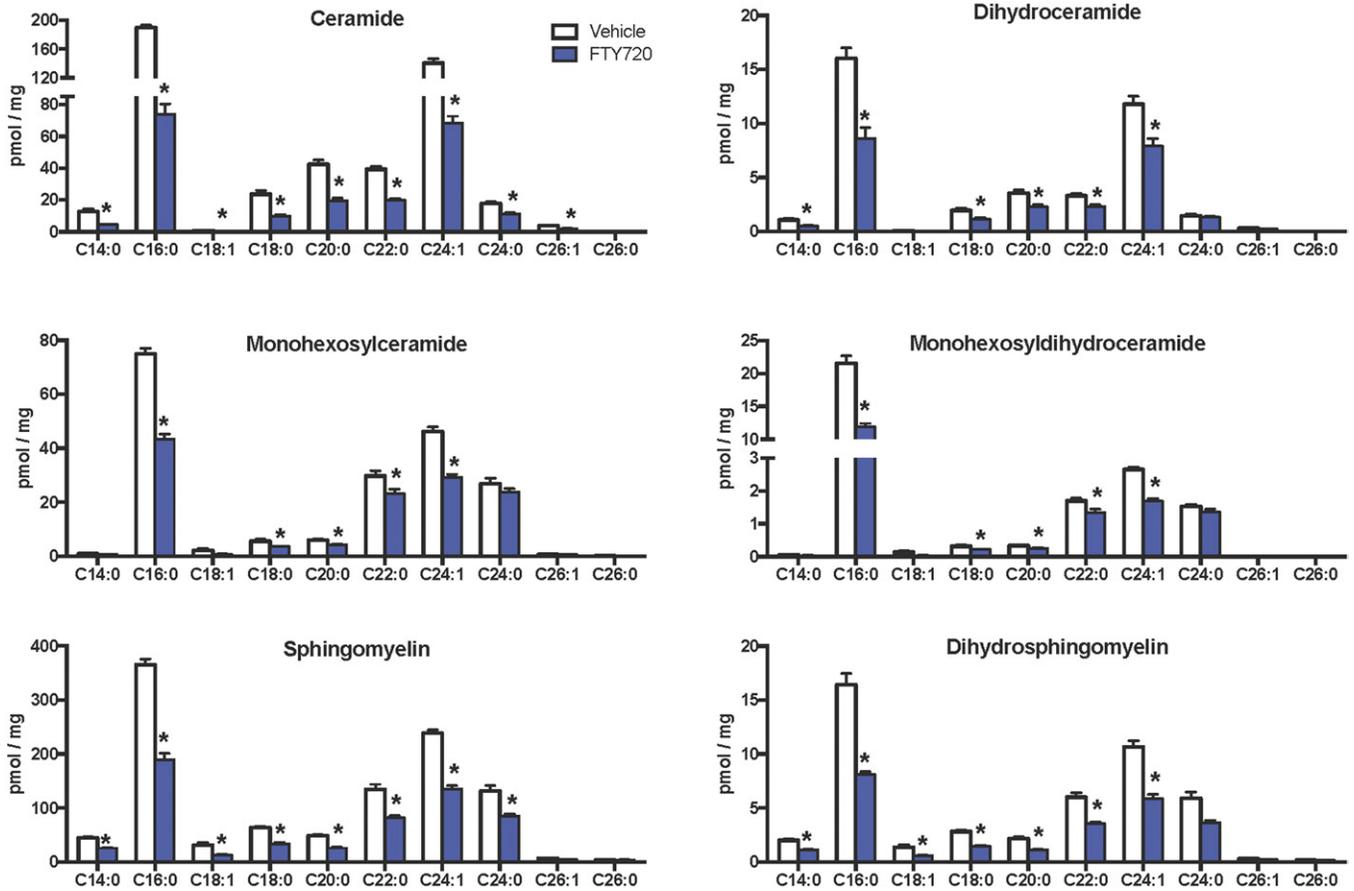
Fig. 5. FTY720 treatment markedly reduced C16:0 sphingolipid species. Mice were fed and treated as described in Fig. 2. Lipids were extracted, and the indicated sphingolipid species were determined by LC/ESI/MS/MS. Numbers indicate chain length followed by the number of double bonds in the fatty acid. Data are means ± SEMs, *n* = 6–11 mice per group. *P < 0.05.

cholesterol homeostasis; acetyl-CoA carboxylase α, which catalyzes the carboxylation of acetyl-CoA to malonyl-CoA, the rate-limiting step in fatty acid synthesis; carnitine palmitoyltransferase 1A, which is involved in β-oxidation of long-chain fatty acids; and peroxisome proliferator-activated receptor γ and its coactivator, which regulate genes involved in energy metabolism (**Fig. 8A**). However, mRNA of Fasn, a key enzyme of de novo fatty acid biosynthesis that catalyzes the synthesis of palmitate from acetyl-CoA and malonyl-CoA, was significantly reduced by FTY720 administration (Fig. 8A).

Fasn expression in NAFLD livers correlated with the degree of hepatic steatosis, but not with inflammation or ballooning of hepatocytes (49). Similar to previous reports (26, 49, 50), there was a significant increase in the expression of Fasn in DIAMOND mice fed a WD with SW compared with a CD (Fig. 8B). FTY720 did not affect Fasn mRNA levels in mice fed a CD; nevertheless, it prevented the increase induced by WD and SW (Fig. 8A, B). Consistent with the effects on mRNA expression, FASN protein levels were also decreased by FTY720 treatment (Fig. 8C).
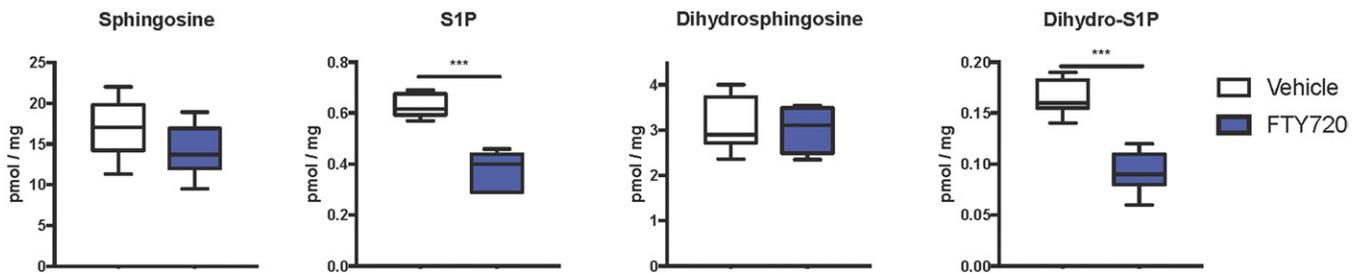
Fig. 6. FTY720 treatment markedly reduced hepatic S1P and dihydro-S1P. Mice were fed and treated as described in Fig. 2. Lipids were extracted, and sphingoid bases and their phosphorylated products were determined by LC/ESI/MS/MS. Data are shown as box and whisker plots, *n* = 6–11 mice per group. ***P < 0.005.
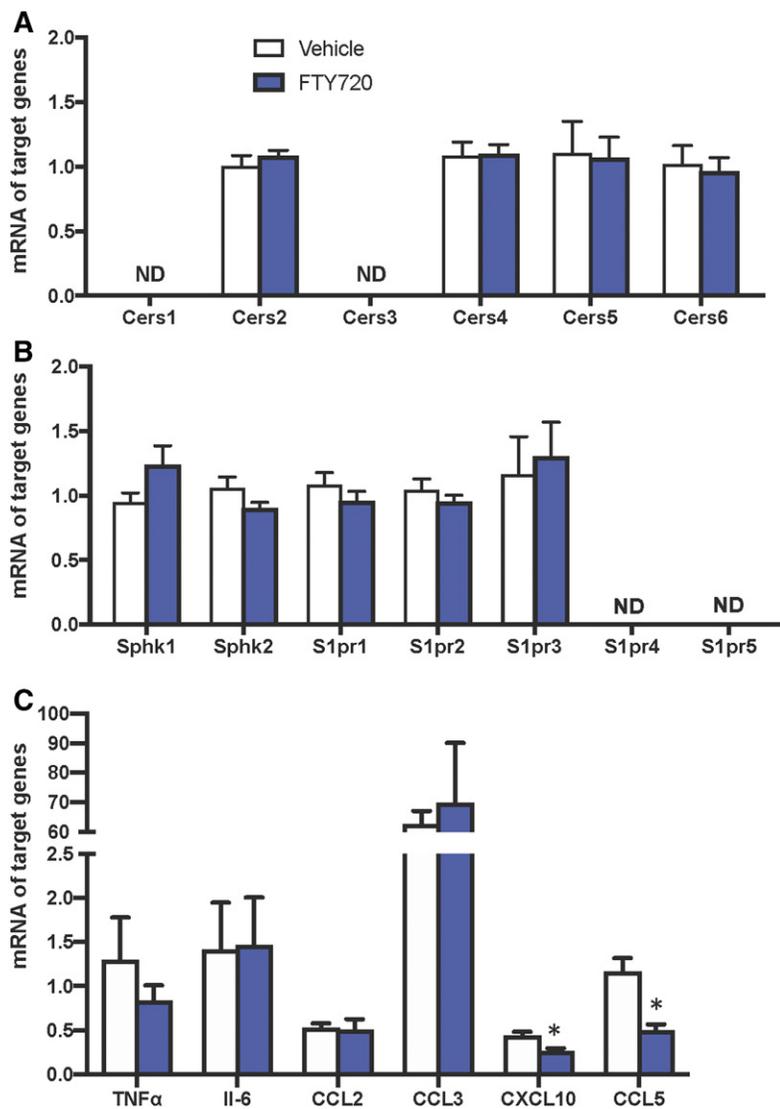
Fig. 7. Effects of FTY720 on the expression of sphingolipid metabolic genes, S1PRs, cytokines, and chemokines. Mice were treated as described in Fig. 2, livers were isolated, and mRNA levels of *Cers1-6* genes (A), *Sphk1, Sphk2,* and *S1pr1-5* genes (B), and cytokine and chemokine genes were determined by quantitative PCR and normalized to *Gapdh.* Data are means ± SEMs, $n = 5$–6 mice per group. $*P < 0/05$. ND, not detected.

We next sought to examine how FTY720 treatment can regulate Fasn expression. Although *FASN* is usually regulated by the Akt/mTORC1 signaling pathway and upregulation of SREBP-1c, which transcriptionally activates *FASN* (51, 52), this pathway is unlikely to be involved in the effects of FTY720. First, FTY720 had no effect on the expression of Srebp-1c (Fig. 8A). Second, activation of Akt as determined by its phosphorylation was not altered by FTY720 (Fig. 8C). FASN expression can also be controlled by histone acetylation and epigenetic regulation (50, 53–55). Because histone deacetylase (HDAC) inhibitors reduce the expression of Fasn (53, 54) and we have found that the phosphorylated active form of FTY720, FTY720-P, which accumulates in the nucleus, similar to nuclear S1P (56), is a potent class I HDAC inhibitor (40, 57), it was also of interest to examine this possibility. Concomitant with the decrease in the expression of FASN at both mRNA and the protein the levels (Fig. 8A–C), FTY720 treatment led to accumulation of FTY720-P in the liver (Fig. 8D). FTY720 administration also dramatically increased histone H3K9 acetylation in the livers of DIAMOND mice fed WD + SW (Fig. 8E), consistent with reduced HDAC activity. Taken together, our results suggest that in addition to decreasing hepatic sphingolipids, FTY720 treatment also decreases FASN expression.

DISCUSSION

NAFLD is a complex disease that is closely associated with obesity (6, 58). In the prevailing "two-hit hypothesis" for the development of NAFLD pathogenesis (59), the "first hit" is due to obesity and insulin resistance, which then increases the susceptibility of the liver to various "second hits," such as oxidative stress and the production of inflammatory cytokines, and, more recently, to the accumulation of ceramides and S1P (12, 13). The prevalence of NAFLD is increasing in the United States, and currently there is no pharmaceutical cure (6). Furthermore, NAFLD has emerged as a leading indication for liver transplants and has contributed to the rising incidence of liver cancer (2).

In this work, we examined the effects of the prodrug FTY720/fingolimod, now used for the treatment of multiple sclerosis, in a diet-induced mouse model of NAFLD
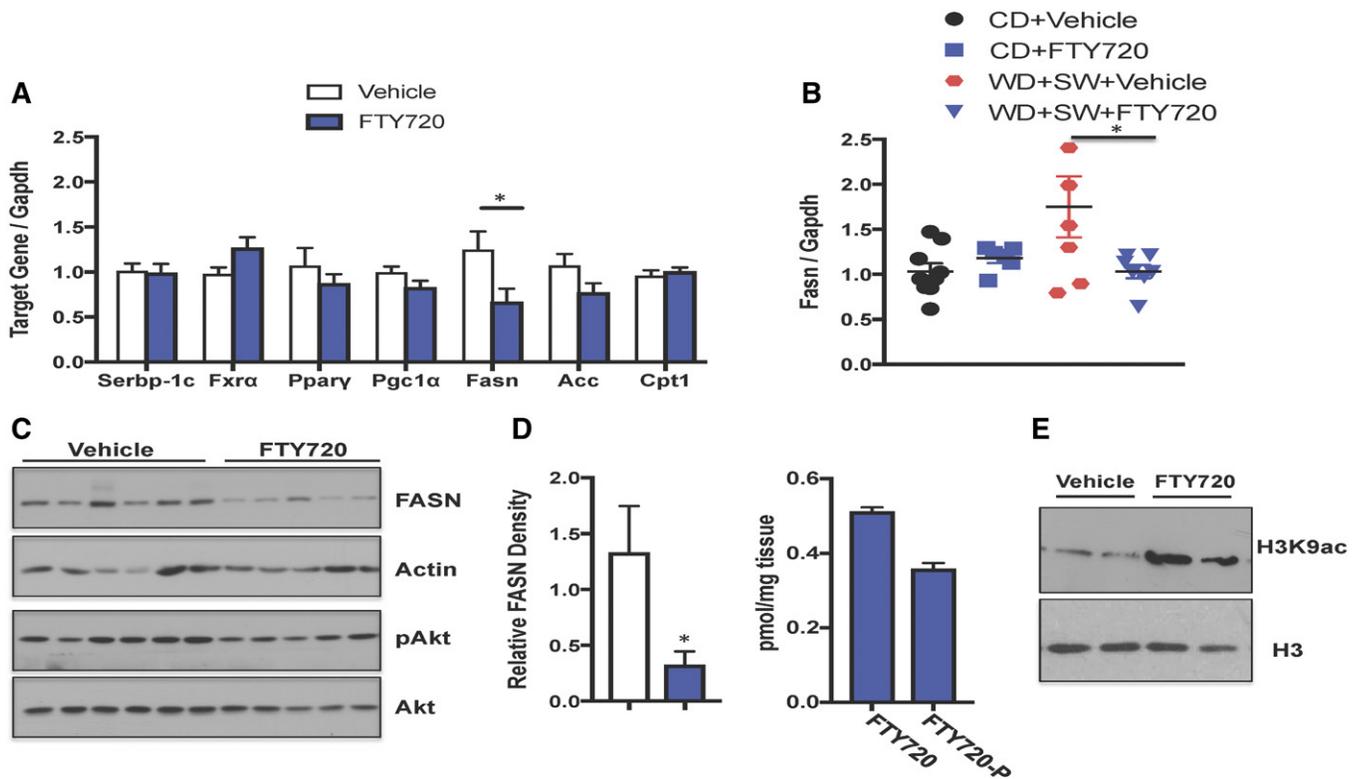
Fig. 8. FTY720 administration decreased HFD-induced FASN expression. B6/129 female mice fed a CD or WD with SW for 16 weeks were treated 3 times per week with vehicle or 0.3 mg/kg FTY720 by gavage as indicated. A, B: Liver mRNA levels of the indicated genes were determined by quantitative PCR and normalized to Gapdh. Data are means ± SEMs. *$P < 0.05$ versus vehicle-treated mice. C: Proteins in liver extracts were analyzed by immunoblot analysis with the indicated antibodies. Blots were stripped and reprobed with anti-actin antibody to show equal loading and transfer. Blots were quantitated by densitometry. Data are means ± SEMs, $n = 5–6$ mice per group. *$P < 0.05$. D: FTY720 and FTY720-P levels in livers from mice fed a WD with SW for 16 weeks and treated with FTY720 were measured by LC/ESI/MS/MS. Data are means ± SEMs. E: Histone H3K9 acetylation in nuclear extracts from livers was determined by immunoblotting with antibodies specific to H3K9 and with anti-histone H3 antibody.

that mimics the hallmarks of the human disease (26). The oral administration of FTY720 to DIAMOND mice attenuated increases in overall body and liver weight, improved glucose tolerance, decreased hepatic triglycerides, and reduced steatosis. FTY720 is structurally similar to the fungal metabolite myriocin and has been shown to decrease de novo ceramide production by inhibiting CerS (29, 30). Indeed, after treating DIAMOND mice with FTY720, there were also significant reductions of hepatic sphingolipids, including ceramides, monohexosylceramides, and sphingomyelins, their dihydro species, as well as S1P. In this regard, it is important to mention that many of these sphingolipids have been implicated in mice models of hepatic steatosis. For example, pharmacological inhibition of glucosylceramide synthase or the genetic depletion of acid sphingomyelinase reduce hepatic triglyceride levels in mice susceptible to the development of a fatty liver (60). Our findings are consistent with studies showing that the administration of myriocin, an inhibitor of serine palmitoyltransferase, the rate-limiting enzyme in de novo ceramide biosynthesis, not only reduced elevation of hepatic ceramide but also suppressed steatosis in different animal models of NAFLD (61, 62). However, while myriocin is highly toxic to humans, FTY720 is already approved for use in humans. As with any medication, FTY720 also has

dose-dependent adverse side effects and toxicity. The immunosuppressive effects of FTY720 increase risks of infections. Bradycardia associated with its administration to multiple sclerosis patients is only observed after the first dose and is manageable. In general, only low rates of long-term drug-related adverse effects have been observed with FTY720 (63).

Combining our findings with previous work suggests that mitigating ceramide levels may serve as an effective method for improving NAFLD pathology. The molecular mechanisms by which increased ceramide contributes to NAFLD development are not completely clear, although several possibilities have been suggested. Utilizing CerS2-null mice that cannot synthesize very-long acyl-chain (C22–C24) ceramides, it was shown that hepatic fatty acid uptake via CD36/FAT can be regulated by altering the acyl-chain composition of sphingolipids (64). Additionally, ceramide perpetuates NAFLD development by increasing hepatic fatty acid levels, promoting inflammation and oxidative stress, along with triggering mitochondrial dysfunction (13, 65). C16-ceramide also mitigates the insulin receptor/Akt signaling pathway and thus decreases fat utilization as an energy source by β-oxidation (17, 66). Mechanistic studies revealed that increases in C16-ceramide caused impaired mitochondrial β-oxidation resulting from the inactivation

of electron transport chain components (19). In agreement, Bruning and colleagues identified *CerS6* and C16-ceramide as a negative regulator of β-oxidative capacity in brown adipose tissue and liver. However, these effects appeared to be independent of increases in respiratory chain capacity in contrast to another report (67). In this regard, daily administration of a selective inhibitor of CerS1, the enzyme that produces C18-ceramide, to mice fed an HFD increased fatty acid oxidation in skeletal muscle and impeded increases in muscle triglycerides and adiposity but did not protect against HFD-induced insulin resistance (68).

In agreement with our work, it was previously reported that the administration of FTY720 during the last 2 weeks of feeding C57BL/6 male mice a diet high in fructose, saturated fat, and cholesterol for 22 weeks decreased steatosis and triglyceride accumulation (46). However, the reduction in liver injury was accompanied by reduced inflammation, likely due to a reduction in hepatic macrophage accumulation without affecting hepatic sphingolipids, whereas in our model, FTY720 only had a minimal effect on inflammation. Nevertheless, FTY720 reduced the expression of the chemokines CXCL10 and CCL5 that have been shown to play a role in liver fibrosis (69). Importantly, we also observed that FTY720 strongly decreased many sphingolipid species. Here, we also made the interesting observation that FTY720 administration to DIAMOND mice reduces their increased expression of FASN, the rate-limiting and last step in de novo fatty acid biosynthesis (70). The main function of FASN is to catalyze the synthesis of palmitate (16:0) that is used for both triglyceride synthesis and the de novo biosynthesis of ceramide. Thus, FASN mRNA and protein expression suppression by FTY720 may be responsible for the reduction in hepatic triglycerides and ceramides we observed in DIAMOND mice.

The transcriptional regulation of *FASN* induced by HFD has been extensively studied, and SREBP-1c and Sp1, which interact and mediate sterol-induced *FASN* expression synergistically, have been identified as key transcription factors, whereas carbohydrate responsive element binding protein appears to be the main regulator of glucose-induced FASN expression (51, 52, 71). Nevertheless, we found that FTY720 did not affect SREBP-1c expression. Instead, in accord with the notion that FASN expression can also be controlled by histone acetylation and epigenetic regulation (50, 53–55, 72), our results indicate that reduction of FASN by FTY720 could be due to increased histone acetylation. Consistent with our previous findings that treatment with FTY720 leads to increased accumulation of the phosphorylated active form of FTY720, FTY720-P, in the nucleus which inhibits class I HDACs (56, 57, 73), we observed that FTY720-P accumulated in the liver of FTY720-treated DIAMOND mice and markedly increased histone H3K9 acetylation. Thus, like other HDAC inhibitors (53, 54, 74), reduction in FASN could be due to inhibition of HDACs by FTY720-P and increased H3K9 acetylation. These findings are in agreement with a recent report showing that the expression of Fasn in the liver is associated with increased H3K9 acetylation that modulates the binding of

carbohydrate responsive element binding protein to the promoter/enhancer region of the *Fasn* gene (75).

Excess fatty acids in the liver promote both liver and muscle insulin resistance, which ultimately leads to more accumulation of fatty acids in the liver (76, 77), resulting in progression to NAFLD (78). Patients with hepatic steatosis have elevated levels of FASN compared with healthy individuals (49, 79). Similarly, mice with hepatic steatosis also have higher levels of FASN (26, 49). Despite numerous studies linking the lipogenic pathway to NAFLD, the development of pharmacological inhibitors of FASN has been slow, and no compounds have moved past the preclinical phase (80). Our data suggest that FTY720 deserves consideration as a therapeutic approach that in association with lifestyle interventions would concurrently improve elevated lipogenesis and could have beneficial effects on fatty liver disease and NASH.

REFERENCES

1. Satapathy, S. K., and A. J. Sanyal. 2015. Epidemiology and natural history of nonalcoholic fatty liver disease. *Semin. Liver Dis.* **35:** 221–235.
2. Cohen, J. C., J. D. Horton, and H. H. Hobbs. 2011. Human fatty liver disease: old questions and new insights. *Science.* **332:** 1519–1523.
3. Farrell, G. C., and C. Z. Larter. 2006. Nonalcoholic fatty liver disease: from steatosis to cirrhosis. *Hepatology.* **43:** S99–S112.
4. Farrell, G. C., D. van Rooyen, L. Gan, and S. Chitturi. 2012. NASH is an inflammatory disorder: pathogenic, prognostic and therapeutic implications. *Gut Liver.* **6:** 149–171.
5. Rinella, M. E., and A. J. Sanyal. 2016. Management of NAFLD: a stage-based approach. *Nat. Rev. Gastroenterol. Hepatol.* **13:** 196–205.
6. Loomba, R., and A. J. Sanyal. 2013. The global NAFLD epidemic. *Nat. Rev. Gastroenterol. Hepatol.* **10:** 686–690.
7. Williams, C. D., J. Stengel, M. I. Asike, D. M. Torres, J. Shaw, M. Contreras, C. L. Landt, and S. A. Harrison. 2011. Prevalence of nonalcoholic fatty liver disease and nonalcoholic steatohepatitis among a largely middle-aged population utilizing ultrasound and liver biopsy: a prospective study. *Gastroenterology.* **140:** 124–131.
8. Sanyal, A. J., S. L. Friedman, A. J. McCullough, and L. Dimick-Santos. 2015. Challenges and opportunities in drug and biomarker development for nonalcoholic steatohepatitis: findings and recommendations from an American Association for the Study of Liver Diseases-U.S. Food and Drug Administration Joint Workshop. *Hepatology.* **61:** 1392–1405.
9. Chavez, J. A., and S. A. Summers. 2010. Lipid oversupply, selective insulin resistance, and lipotoxicity: molecular mechanisms. *Biochim. Biophys. Acta.* **1801:** 252–265.
10. Gorden, D. L., D. S. Myers, P. T. Ivanova, E. Fahy, M. R. Maurya, S. Gupta, J. Min, N. J. Spann, J. G. McDonald, S. L. Kelly, et al. 2015. Biomarkers of NAFLD progression: a lipidomics approach to an epidemic. *J. Lipid Res.* **56:** 722–736.
11. Luukkonen, P. K., Y. Zhou, S. Sadevirta, M. Leivonen, J. Arola, M. Oresic, T. Hyotylainen, and H. Yki-Jarvinen. 2016. Hepatic ceramides dissociate steatosis and insulin resistance in patients with nonalcoholic fatty liver disease. *J. Hepatol.* **64:** 1167–1175.
12. Chavez, J. A., and S. A. Summers. 2012. A ceramide-centric view of insulin resistance. *Cell Metab.* **15:** 585–594.
13. Pagadala, M., T. Kasumov, A. J. McCullough, N. N. Zein, and J. P. Kirwan. 2012. Role of ceramides in nonalcoholic fatty liver disease. *Trends Endocrinol. Metab.* **23:** 365–371.
14. Rohrbach, T., M. Maceyka, and S. Spiegel. 2017. Sphingosine kinase and sphingosine-1-phosphate in liver pathobiology. *Crit. Rev. Biochem. Mol. Biol.* **52:** 543–553.
15. Choi, S., and A. J. Snider. 2015. Sphingolipids in high fat diet and obesity-related diseases. *Mediators Inflamm.* **2015:** 520618.

16. Holland, W. L., B. T. Bikman, L. P. Wang, G. Yuguang, K. M. Sargent, S. Bulchand, T. A. Knotts, G. Shui, D. J. Clegg, M. R. Wenk, et al. 2011. Lipid-induced insulin resistance mediated by the pro-inflammatory receptor TLR4 requires saturated fatty acid-induced ceramide biosynthesis in mice. *J. Clin. Invest.* **121:** 1858–1870.

17. Meikle, P. J., and S. A. Summers. 2017. Sphingolipids and phospholipids in insulin resistance and related metabolic disorders. *Nat. Rev. Endocrinol.* **13:** 79–91.

18. Turpin, S. M., H. T. Nicholls, D. M. Willmes, A. Mourier, S. Brodesser, C. M. Wunderlich, J. Mauer, E. Xu, P. Hammerschmidt, H. S. Bronneke, et al. 2014. Obesity-induced CerS6-dependent C16:0 ceramide production promotes weight gain and glucose intolerance. *Cell Metab.* **20:** 678–686.

19. Raichur, S., S. T. Wang, P. W. Chan, Y. Li, J. Ching, B. Chaurasia, S. Dogra, M. K. Ohman, K. Takeda, S. Sugii, et al. 2014. CerS2 haploinsufficiency inhibits beta-oxidation and confers susceptibility to diet-induced steatohepatitis and insulin resistance. *Cell Metab.* **20:** 687–695. [Erratum. 2014. *Cell Metab.* **20:** 919.]

20. Gosejacob, D., P. S. Jager, K. Vom Dorp, M. Frejno, A. C. Carstensen, M. Kohnke, J. Degen, P. Dormann, and M. Hoch. 2016. Ceramide synthase 5 is essential to maintain C16:0-ceramide pools and contributes to the development of diet-induced obesity. *J. Biol. Chem.* **291:** 6989–7003.

21. Bergman, B. C., J. T. Brozinick, A. Strauss, S. Bacon, A. Kerege, H. H. Bui, P. Sanders, P. Siddall, T. Wei, M. K. Thomas, et al. 2016. Muscle sphingolipids during rest and exercise: a C18:0 signature for insulin resistance in humans. *Diabetologia.* **59:** 785–798.

22. Fayyaz, S., J. Henkel, L. Japtok, S. Kramer, G. Damm, D. Seehofer, G. P. Puschel, and B. Kleuser. 2014. Involvement of sphingosine 1-phosphate in palmitate-induced insulin resistance of hepatocytes via the S1P2 receptor subtype. *Diabetologia.* **57:** 373–382.

23. Geng, T., A. Sutter, M. D. Harland, B. A. Law, J. S. Ross, D. Lewin, A. Palanisamy, S. B. Russo, K. D. Chavin, and L. A. Cowart. 2015. SphK1 mediates hepatic inflammation in a mouse model of NASH induced by high saturated fat feeding and initiates proinflammatory signaling in hepatocytes. *J. Lipid Res.* **56:** 2359–2371.

24. Kowalski, G. M., A. L. Carey, A. Selathurai, B. A. Kingwell, and C. R. Bruce. 2013. Plasma sphingosine-1-phosphate is elevated in obesity. *PLoS One.* **8:** e72449.

25. Jacobs, A., A. S. Warda, J. Verbeek, D. Cassiman, and P. Spincemaille. 2016. An overview of mouse models of nonalcoholic steatohepatitis: from past to present. *Curr. Protoc. Mouse Biol.* **6:** 185–200.

26. Asgharpour, A., S. C. Cazanave, T. Pacana, M. Seneshaw, R. Vincent, B. A. Banini, D. P. Kumar, K. Daita, H. K. Min, F. Mirshahi, et al. 2016. A diet-induced animal model of non-alcoholic fatty liver disease and hepatocellular cancer. *J. Hepatol.* **65:** 579–588.

27. Sanyal, A. J., and T. Pacana. 2015. A lipidomic readout of disease progression in a diet-induced mouse model of nonalcoholic fatty liver disease. *Trans. Am. Clin. Climatol. Assoc.* **126:** 271–288.

28. Brinkmann, V., A. Billich, T. Baumruker, P. Heining, R. Schmouder, G. Francis, S. Aradhye, and P. Burtin. 2010. Fingolimod (FTY720): discovery and development of an oral drug to treat multiple sclerosis. *Nat. Rev. Drug Discov.* **9:** 883–897.

29. Lahiri, S., H. Park, E. L. Laviad, X. Lu, R. Bittman, and A. H. Futerman. 2009. Ceramide synthesis is modulated by the sphingosine analog FTY720 via a mixture of uncompetitive and noncompetitive inhibition in an Acyl-CoA chain length-dependent manner. *J. Biol. Chem.* **284:** 16090–16098.

30. Berdyshev, E. V., I. Gorshkova, A. Skobeleva, R. Bittman, X. Lu, S. M. Dudek, T. Mirzapoiazova, J. G. Garcia, and V. Natarajan. 2009. FTY720 inhibits ceramide synthases and up-regulates dihydrosphingosine 1-phosphate formation in human lung endothelial cells. *J. Biol. Chem.* **284:** 5467–5477.

31. Chen, H., J. T. Tran, A. Eckerd, T. P. Huynh, M. H. Elliott, R. S. Brush, and N. A. Mandal. 2013. Inhibition of de novo ceramide biosynthesis by FTY720 protects rat retina from light-induced degeneration. *J. Lipid Res.* **54:** 1616–1629.

32. Stiles, M., H. Qi, E. Sun, J. Tan, H. Porter, J. Allegood, C. E. Chalfant, D. Yasumura, M. T. Matthes, M. M. LaVail, et al. 2016. Sphingolipid profile alters in retinal dystrophic P23H-1 rats and systemic FTY720 can delay retinal degeneration. *J. Lipid Res.* **57:** 818–831.

33. Oyeniran, C., J. L. Sturgill, N. C. Hait, W. C. Huang, D. Avni, M. Maceyka, J. Newton, J. C. Allegood, A. Montpetit, D. H. Conrad, et al. 2015. Aberrant ORM (yeast)-like protein isoform 3 (ORMDL3) expression dysregulates ceramide homeostasis in cells and ceramide exacerbates allergic asthma in mice. *J. Allergy Clin. Immunol.* **136:** 1035–1046.e6.

34. Lim, K. G., F. Tonelli, Z. Li, X. Lu, R. Bittman, S. Pyne, and N. J. Pyne. 2011. FTY720 analogues as sphingosine kinase 1 inhibitors: enzyme inhibition kinetics, allosterism, proteasomal degradation, and actin rearrangment in MCF-7 breast cancer cells. *J. Biol. Chem.* **286:** 18633–18640.

35. Liang, J., M. Nagahashi, E. Y. Kim, K. B. Harikumar, A. Yamada, W. C. Huang, N. C. Hait, J. C. Allegood, M. M. Price, D. Avni, et al. 2013. Sphingosine-1-phosphate links persistent STAT3 activation, chronic intestinal inflammation, and development of colitis-associated cancer. *Cancer Cell.* **23:** 107–120.

36. Norheim, F., S. T. Hui, E. Kulahcioglu, M. Mehrabian, R. M. Cantor, C. Pan, B. W. Parks, and A. J. Lusis. 2017. Genetic and hormonal control of hepatic steatosis in female and male mice. *J. Lipid Res.* **58:** 178–187.

37. Lattouf, R., R. Younes, D. Lutomski, N. Naaman, G. Godeau, K. Senni, and S. Changotade. 2014. Picrosirius red staining: a useful tool to appraise collagen networks in normal and pathological tissues. *J. Histochem. Cytochem.* **62:** 751–758.

38. Kleiner, D. E., E. M. Brunt, M. Van Natta, C. Behling, M. J. Contos, O. W. Cummings, L. D. Ferrell, Y. C. Liu, M. S. Torbenson, A. Unalp-Arida, M., et al. 2005. Design and validation of a histological scoring system for nonalcoholic fatty liver disease. *Hepatology.* **41:** 1313–1321.

39. Andrikopoulos, S., A. R. Blair, N. Deluca, B. C. Fam, and J. Proietto. 2008. Evaluating the glucose tolerance test in mice. *Am. J. Physiol. Endocrinol. Metab.* **295:** E1323–E1332.

40. Hait, N. C., J. Allegood, M. Maceyka, G. M. Strub, K. B. Harikumar, S. K. Singh, C. Luo, R. Marmorstein, T. Kordula, S. Milstien, et al. 2009. Regulation of histone acetylation in the nucleus by sphingosine-1-phosphate. *Science.* **325:** 1254–1257.

41. Cai, L., C. Oyeniran, D. D. Biwas, J. Allegood, S. Milstien, T. Kordula, M. Maceyka, and S. Spiegel. 2016. ORMDL proteins regulate ceramide levels during sterile inflammation. *J. Lipid Res.* **57:** 1412–1422.

42. Charlton, M., A. Krishnan, K. Viker, S. Sanderson, S. Cazanave, A. McConico, H. Masuoko, and G. Gores. 2011. Fast food diet mouse: novel small animal model of NASH with ballooning, progressive fibrosis, and high physiological fidelity to the human condition. *Am. J. Physiol. Gastrointest. Liver Physiol.* **301:** G825–G834.

43. Bruce, C. R., S. Risis, J. R. Babb, C. Yang, R. S. Lee-Young, D. C. Henstridge, and M. A. Febbraio. 2013. The sphingosine-1-phosphate analog FTY720 reduces muscle ceramide content and improves glucose tolerance in high fat-fed male mice. *Endocrinology.* **154:** 65–76.

44. Martínez, L., S. Torres, A. Baulies, C. Alarcon-Vila, M. Elena, G. Fabrias, J. Casas, J. Caballeria, J. C. Fernandez-Checa, and C. Garcia-Ruiz. 2015. Myristic acid potentiates palmitic acid-induced lipotoxicity and steatohepatitis associated with lipodystrophy by sustaing de novo ceramide synthesis. *Oncotarget.* **6:** 41479–41496.

45. Li, C., X. Jiang, L. Yang, X. Liu, S. Yue, and L. Li. 2009. Involvement of sphingosine 1-phosphate (SIP)/S1P3 signaling in cholestasis-induced liver fibrosis. *Am. J. Pathol.* **175:** 1464–1472.

46. Mauer, A. S., P. Hirsova, J. L. Maiers, V. H. Shah, and H. Malhi. 2017. Inhibition of sphingosine 1-phosphate signaling ameliorates murine nonalcoholic steatohepatitis. *Am. J. Physiol. Gastrointest. Liver Physiol.* **312:** G300–G313.

47. Braunersreuther, V., G. L. Viviani, F. Mach, and F. Montecucco. 2012. Role of cytokines and chemokines in non-alcoholic fatty liver disease. *World J. Gastroenterol.* **18:** 727–735.

48. Hassan, K., V. Bhalla, M. E. El Regal, and H. H. A-Kader. 2014. Nonalcoholic fatty liver disease: a comprehensive review of a growing epidemic. *World J. Gastroenterol.* **20:** 12082–12101.

49. Dorn, C., M. O. Riener, G. Kirovski, M. Saugspier, K. Steib, T. S. Weiss, E. Gabele, G. Kristiansen, A. Hartmann, and C. Hellerbrand. 2010. Expression of fatty acid synthase in nonalcoholic fatty liver disease. *Int. J. Clin. Exp. Pathol.* **3:** 505–514.

50. Suzuki, T., T. Muramatsu, K. Morioka, T. Goda, and K. Mochizuki. 2015. ChREBP binding and histone modifications modulate hepatic expression of the Fasn gene in a metabolic syndrome rat model. *Nutrition.* **31:** 877–883.

51. Magaña, M. M., and T. F. Osborne. 1996. Two tandem binding sites for sterol regulatory element binding proteins are required for sterol regulation of fatty-acid synthase promoter. *J. Biol. Chem.* **271:** 32689–32694.

52. Horton, J. D., J. L. Goldstein, and M. S. Brown. 2002. SREBPs: activators of the complete program of cholesterol and fatty acid synthesis in the liver. *J. Clin. Invest.* **109:** 1125–1131.

53. Chittur, S. V., N. Sangster-Guity, and P. J. McCormick. 2008. Histone deacetylase inhibitors: a new mode for inhibition of cholesterol metabolism. *BMC Genomics.* **9:** 507.

54. Brina, D., A. Miluzio, S. Ricciardi, K. Clarke, P. K. Davidsen, G. Viero, T. Tebaldi, N. Offenhauser, J. Rozman, B. Rathkolb, et al. 2015. eIF6 coordinates insulin sensitivity and lipid metabolism by coupling translation to transcription. *Nat. Commun.* **6:** 8261.

55. Du, X., C. Cai, J. Yao, Y. Zhou, H. Yu, and W. Shen. 2017. Histone modifications in FASN modulated by sterol regulatory element-binding protein 1c and carbohydrate responsive-element binding protein under insulin stimulation are related to NAFLD. *Biochem. Biophys. Res. Commun.* **483:** 409–417.

56. Hait, N. C., D. Avni, A. Yamada, M. Nagahashi, T. Aoyagi, H. Aoki, C. I. Dumur, Z. Zelenko, E. J. Gallagher, D. Leroith, et al. 2015. The phosphorylated prodrug FTY720 is a histone deacetylase inhibitor that reactivates ERalpha expression and enhances hormonal therapy for breast cancer. *Oncogenesis.* **4:** e156.

57. Hait, N. C., L. E. Wise, J. C. Allegood, M. O'Brien, D. Avni, T. M. Reeves, P. E. Knapp, J. Lu, C. Luo, M. F. Miles, et al. 2014. Active, phosphorylated fingolimod inhibits histone deacetylases and facilitates fear extinction memory. *Nat. Neurosci.* **17:** 971–980.

58. Angulo, P. 2002. Nonalcoholic fatty liver disease. *N. Engl. J. Med.* **346:** 1221–1231.

59. Buzzetti, E., M. Pinzani, and E. A. Tsochatzis. 2016. The multiple-hit pathogenesis of non-alcoholic fatty liver disease (NAFLD). *Metabolism.* **65:** 1038–1048.

60. Bikman, B. T., and S. A. Summers. 2011. Sphingolipids and hepatic steatosis. *Adv. Exp. Med. Biol.* **721:** 87–97.

61. Kurek, K., D. M. Piotrowska, P. Wiesiolek-Kurek, B. Lukaszuk, A. Chabowski, J. Gorski, and M. Zendzian-Piotrowska. 2014. Inhibition of ceramide de novo synthesis reduces liver lipid accumulation in rats with nonalcoholic fatty liver disease. *Liver Int.* **34:** 1074–1083.

62. Kasumov, T., L. Li, M. Li, K. Gulshan, J. P. Kirwan, X. Liu, S. Previs, B. Willard, J. D. Smith, and A. McCullough. 2015. Ceramide as a mediator of non-alcoholic fatty liver disease and associated atherosclerosis. *PLoS One.* **10:** e0126910.

63. Comi, G., H. P. Hartung, R. Bakshi, I. M. Williams, and H. Wiendl. 2017. Benefit-risk profile of sphingosine-1-phosphate receptor modulators in relapsing and secondary progressive multiple sclerosis. *Drugs.* **77:** 1755–1768.

64. Park, J. W., W. J. Park, and A. H. Futerman. 2014. Ceramide synthases as potential targets for therapeutic intervention in human diseases. *Biochim. Biophys. Acta.* **1841:** 671–681.

65. Marí, M., and J. C. Fernandez-Checa. 2007. Sphingolipid signalling and liver diseases. *Liver Int.* **27:** 440–450.

66. Smith, M. E., T. S. Tippetts, E. S. Brassfield, B. J. Tucker, A. Ockey, A. C. Swensen, T. S. Anthonymuthu, T. D. Washburn, D. A. Kane, J. T. Prince, et al. 2013. Mitochondrial fission mediates ceramide-induced metabolic disruption in skeletal muscle. *Biochem. J.* **456:** 427–439.

67. Zigdon, H., A. Kogot-Levin, J. W. Park, R. Goldschmidt, S. Kelly, A. H. Merrill, Jr., A. Scherz, Y. Pewzner-Jung, A. Saada, and A. H. Futerman. 2013. Ablation of ceramide synthase 2 causes chronic oxidative stress due to disruption of the mitochondrial respiratory chain. *J. Biol. Chem.* **288:** 4947–4956.

68. Turner, N., X. Y. Lim, H. D. Toop, B. Osborne, A. E. Brandon, E. N. Taylor, C. E. Fiveash, H. Govindaraju, J. D. Teo, H. P. McEwen, et al. 2018. A selective inhibitor of ceramide synthase 1 reveals a novel role in fat metabolism. *Nat. Commun.* **9:** 3165.

69. Marra, F., and F. Tacke. 2014. Roles for chemokines in liver disease. *Gastroenterology.* **147:** 577–594.

70. Chirala, S. S., and S. J. Wakil. 2004. Structure and function of animal fatty acid synthase. *Lipids.* **39:** 1045–1053.

71. Jensen-Urstad, A. P., and C. F. Semenkovich. 2012. Fatty acid synthase and liver triglyceride metabolism: housekeeper or messenger? *Biochim. Biophys. Acta.* **1821:** 747–753.

72. Gao, X., S. H. Lin, F. Ren, J. T. Li, J. J. Chen, C. B. Yao, H. B. Yang, S. X. Jiang, G. Q. Yan, D. Wang, et al. 2016. Acetate functions as an epigenetic metabolite to promote lipid synthesis under hypoxia. *Nat. Commun.* **7:** 11960.

73. Newton, J., N. C. Hait, M. Maceyka, A. Colaco, M. Maczis, C. A. Wassif, A. Cougnoux, F. D. Porter, S. Milstien, N. Platt, et al. 2017. FTY720/fingolimod increases NPC1 and NPC2 expression and reduces cholesterol and sphingolipid accumulation in Niemann-Pick type C mutant fibroblasts. *FASEB J.* **31:** 1719–1730.

74. Kim, M., H. A. Lee, H. M. Cho, S. H. Kang, E. Lee, and I. K. Kim. 2018. Histone deacetylase inhibition attenuates hepatic steatosis in rats with experimental Cushing's syndrome. *Korean J. Physiol. Pharmacol.* **22:** 23–33.

75. Cai, C., H. Yu, G. Huang, X. Du, X. Yu, Y. Zhou, and W. Shen. 2018. Histone modifications in fatty acid synthase modulated by carbohydrate responsive element binding protein are associated with nonalcoholic fatty liver disease. *Int. J. Mol. Med.* **42:** 1215–1228.

76. Fabbrini, E., S. Sullivan, and S. Klein. 2010. Obesity and nonalcoholic fatty liver disease: biochemical, metabolic, and clinical implications. *Hepatology.* **51:** 679–689.

77. Starley, B. Q., C. J. Calcagno, and S. A. Harrison. 2010. Nonalcoholic fatty liver disease and hepatocellular carcinoma: a weighty connection. *Hepatology.* **51:** 1820–1832.

78. Koo, S. H. 2013. Nonalcoholic fatty liver disease: molecular mechanisms for the hepatic steatosis. *Clin. Mol. Hepatol.* **19:** 210–215.

79. Mitsuyoshi, H., K. Yasui, Y. Harano, K. Endo, K. Tsuji, M. Minami, Y. Itoh, T. Okanoue, and T. Yoshikawa. 2009. Analysis of hepatic genes involved in the metabolism of fatty acids and iron in nonalcoholic fatty liver disease. *Hepatol. Res.* **39:** 366–373.

80. Angeles, T. S., and R. L. Hudkins. 2016. Recent advances in targeting the fatty acid biosynthetic pathway using fatty acid synthase inhibitors. *Expert Opin. Drug Discov.* **11:** 1187–1199.